



HAL
open science

A simple bidirectionnal reflectance model for terrestrial surfaces

Bernard Pinty, D. Ramond

► **To cite this version:**

Bernard Pinty, D. Ramond. A simple bidirectionnal reflectance model for terrestrial surfaces. Journal of Geophysical Research, 1986. hal-01982365

HAL Id: hal-01982365

<https://uca.hal.science/hal-01982365>

Submitted on 16 Mar 2021

HAL is a multi-disciplinary open access archive for the deposit and dissemination of scientific research documents, whether they are published or not. The documents may come from teaching and research institutions in France or abroad, or from public or private research centers.

L'archive ouverte pluridisciplinaire **HAL**, est destinée au dépôt et à la diffusion de documents scientifiques de niveau recherche, publiés ou non, émanant des établissements d'enseignement et de recherche français ou étrangers, des laboratoires publics ou privés.

A Simple Bidirectional Reflectance Model for Terrestrial Surfaces

B. PINTY AND D. RAMOND

Laboratoire Associé de Météorologie Physique/Institut et Observatoire de Physique du Globe, Université de Clermont
Laboratoire Associé au Centre National de la Recherche Scientifique, Aubière, France

A simple bidirectional reflectance model is derived for terrestrial surfaces. This model uses photometric relationships together with data from the Nimbus 7 Earth Radiation Budget (ERB) Experiment. It is shown that the model provides a good description of bidirectional patterns derived from satellite observations for two classes of broad uniform surfaces, namely, land and desert. Dependency of the derived albedo model on solar zenith angle is also studied and compared with several observations made at the surface of the earth. Despite the simplicity of the approach the proposed bidirectional reflectance model might be useful for several applications in satellite remote sensing.

1. INTRODUCTION

The suitability of satellite measurements for accurate earth radiation budget assessments is limited by the possibility of inferring flux quantities from a single-angle observation at the top of the atmosphere. Indeed, radiances measured by narrow field of view instruments depend on the geometry of illumination and observation, namely, the solar zenith angle, the satellite viewing angle, and the relative azimuth angle between the two optical paths [Ruff *et al.*, 1968]. Thus the angular distribution of radiances with respect to observational geometry must be known in order to estimate the instantaneous albedo for a given solar angle [Stephens *et al.*, 1981]. Simultaneously, since daily values are desirable for the earth radiation budget [Raschke *et al.*, 1973], the variation of the instantaneous albedo with solar zenith angle is also needed. At a climatic scale the bidirectional reflectance patterns derived from the Nimbus 7 Earth Radiation Budget (ERB) Experiment constitute a valuable data base [Barkstrom, 1984; Jacobowitz *et al.*, 1984]. Patterns of bidirectional reflectance deduced from Nimbus 7 data show that the Lambertian hypothesis is unacceptable for several surface types, even when considered on a large spatial scale.

The behavior of the angular distribution of the energy reflected by the earth is not yet predicted by models where the reflector types and the geometric conditions are the input parameters. However, such models have been developed for the study of bidirectional reflectance patterns of the moon and other planets of the solar system [Minnaert, 1941; Hapke, 1963; Thorpe, 1977]. These models are based on semiempirical illumination laws and simultaneously involve the satisfaction of simple optical laws such as the reciprocity principle [Minnaert, 1941]. Basically, the anisotropy problem intervening in satellite remote sensing of the earth surface is the same as the one intervening in photometric studies of other planets. Nevertheless, only a very few attempts have been made to use such photometric relationships in studying the earth by satellite [Gillespie and Kahle, 1977; Smith *et al.*, 1980].

Our purpose is to adapt a bidirectional model developed for lunar and Martian surfaces to observations of the earth by satellites. The present investigation is limited to the study of terrestrial surfaces (land and desert) which constitute a part of the Nimbus 7 data file. Section 2 is devoted to the construction of a simple bidirectional model for land and desert sur-

face types. The agreement between this model and surface measurements is discussed in the last section.

2. CONSTRUCTION OF A BIDIRECTIONAL REFLECTANCE MODEL FOR TERRESTRIAL SURFACES

2.1. Anisotropic Factors

According to the well-known study by Raschke *et al.* [1973], the measured instantaneous albedos are usually expressed with the help of anisotropic factors:

$$a_p(i) = \frac{1}{E_0 \cos i} [\Pi L_S(i, e, \psi) / f(i, e, \psi)] \quad (1)$$

with

$$f(i, e, \psi) = \Pi L_S(i, e, \psi) / \int_0^{2\pi} \int_0^{\pi/2} L_S(i, e, \psi) \cos e \sin e \, de \, d\psi \quad (2)$$

where $a_p(i)$ is the instantaneous albedo, E_0 the terrestrial solar irradiance, L_S the radiance measured by the satellite, i and e the solar zenith angle and the satellite viewing angle, respectively, and ψ the relative azimuth between the two optical paths.

According to (2), the anisotropic factor $f(i, e, \psi)$ can be defined as the ratio of the "isotropic irradiance" to the integrated anisotropic radiance. Thus the anisotropic factor is equal to 1.0 for isotropic materials and any departure from 1.0 represents the intrinsic anisotropy of the sensed medium. The chief advantage of (1) lies in the fact that the anisotropic factors can be estimated from long-time series of Nimbus 7 data which allow a numerical computation of the integrated anisotropic radiance. Proceeding this way, Taylor and Stowe [1984a] have obtained the anisotropic factors for eight uniform surface types; their classification separates land, desert, ocean, and snow regions under clear and cloudy conditions.

The monochromatic radiance L_S at the top of a cloud free atmosphere over a flat homogeneous terrain can be written as

$$L_S(i, e, \psi) = L_a(i, e, \psi) + \frac{1}{\Pi} E_0 \cos i Td(i) Td(e) \cdot [\rho(i, e, \psi) + a(i)r(i)][1 + r(e)] \quad (3)$$

where L_a denotes the upwelling sky radiance, Td the direct transmittance, r the ratio of diffuse over direct transmittance, ρ the bidirectional reflectance of the surface, and a the directional hemispherical reflectance of the surface which is equal

Copyright 1986 by the American Geophysical Union.

Paper number 6D0165.
0148-0227/86/006D-0165\$05.00

to the integral of the directional reflectance over all reflection angles and azimuths divided by Π . Note that the effect of multiple scattering between the ground and the atmosphere is neglected in (3).

The bidirectional radiance and the anisotropic factors may be obtained explicitly from (2), (3), and (4) if the appropriate parameters describing the optical properties of the atmosphere and of the surface are known. This is not easy for the present, mainly because the bidirectional properties of the surfaces are still poorly known at the spatial scales convenient for earth radiation budget investigations. However, using the anisotropic factors from the Nimbus 7 ERB experiment as an input parameter and using average atmospheric functions a priori given, it is possible to search for an analytical expression of the surface reflectances which ensures a good fit of the anisotropic factors obtained under clear-sky conditions. Obviously, this approach assumes that it is possible to describe the contribution of the atmosphere in the Nimbus 7 data base through a set of averaged optical parameters corresponding to typical clear-sky atmospheric functions. In some ways the choice of such a crude modelization of the atmosphere means that the anisotropy is mainly controlled by the reflection functions of the underlying surfaces. Although (3) is defined for monochromatic quantities, we will reduce the complexity of our approach by using functions averaged over the entire solar spectrum to estimate the broadband radiances. In the following discussion it must be kept in mind that this simplifying approximation introduces an error in the estimate of the masking effect of the atmosphere.

2.2. Atmospheric Functions

As mentioned above, the present investigation is limited to cloudless and dust free cases. Assuming conservative single scattering, the upwelling radiance is obtained from the following expression:

$$L_a(i, e, \psi) = \frac{E_0 \cos i}{\cos i + \cos e} \frac{P(\xi a)}{4\Pi} \cdot \{1 - \exp[-\tau(m(i) + m(e))]\} \quad (4)$$

where τ is the total extinction coefficient, m the relative air mass taken from *Kasten* [1966], ξa the scattering angle, and P the single-scattering phase function. For an atmosphere scattering with a Rayleigh directional distribution, $P(\xi a)$ is given by (5):

$$P(\xi a) = \frac{3}{4}[1 + \cos^2(\xi a)] \quad (5)$$

The product of the direct transmittance factors in (3) becomes:

$$Td(i)Td(e) = \exp\{-\tau[m(i) + m(e)]\} \quad (6)$$

The ratio of diffuse to direct transmittance has complex functional dependencies, mainly with respect to the total optical depth, the ground albedo, and the solar zenith angle [*King and Herman*, 1979]. Here again we made a simplifying approximation by considering that this ratio is only dependent on the solar zenith angle for low to intermediate ground albedo and for low optical depth. The functional dependency upon the solar angle for angles less than 70° has been obtained from a numerical interpolation of the results presented by *Braslau and Dave* [1973] for an atmosphere including Rayleigh scattering plus gas absorption. An investigation of lower sun conditions would require a more sophisticated treatment, since under such angular conditions a large amount of the total illumination comes from the diffuse radiation.

2.3. Bidirectional Surface Model

Using semiempirical photometric relationships, together with the reciprocity principle, *Minnaert* [1941] has proposed the following equation for lunar surface reflectances:

$$\rho_0(i, e, \psi) = \rho_0 \cos^{k-1}(i) \cos^{k-1}(e) \quad (7)$$

where ρ_0 is the reflectance for overhead sun and nadir observation, and k is a parameter varying typically between 0 and 1.0 for lunar surfaces.

Equation (7) gives the dependency of the reflectance not only upon geometrical conditions but also upon the physical state of the surface through the k parameter. From this equation it appears that the k parameter is equal to 1.0 for isotropic surfaces, whereas intermediate values of k describe a departure from this case. From laboratory experiments, *Hapke and Van Horn* [1963] have illustrated the variation of the k parameter with the actual surface roughness of the sensed surface. Under small phase angle conditions, several authors have shown that (7) is able to account for observational results from moon and Mars surfaces (see, for example, *O'Leary and Briggs* [1970]; *Young and Collins* [1971]; *Thorpe* [1977]; *Kieffer et al.* [1977]). However, in (7) the dependency of reflectance with the phase angle is omitted. From theoretical studies, *Hapke* [1963] and *Veverka and Wasserman* [1972] have expressed this last angular dependency of the surface reflectance in some specific cases. More recently, using a best fit technique, *Kieffer et al.* [1977] and *Thorpe* [1977] have taken into account the variation of the reflectance with the phase angle for some Martian regions observed during the Viking mission. The phase angle ξ is related to the relative azimuth by:

$$\cos \xi = \cos i \cos e + \sin i \sin e \cos \psi \quad (8)$$

Depending on the nature and on the geometrical arrangement of the elements making up the surface, all reflectors must belong to one of the four following categories according to their indicatrix scattering shape: orthotropic (isotropic scattering), specular (large scattering in the direction of specular reflection), pitted (predominantly backward scattering), mixed (minimum scattering near the normal to the surface). With regard to the broad classification of terrestrial surfaces used by *Taylor and Stowe* [1984a] for the whole earth, it can be thought intuitively that land and desert surface types belong to the third or the fourth categories mentioned.

With the limitations mentioned above and using a *Minnaert* characterization for the surface, the bidirectional radiance reaching the satellite can be expressed as follows:

$$L_S(i, e, \psi) = B \left\{ A [1 + \cos^2(\xi a)] \frac{\cos i}{\cos i + \cos e} \cdot [1 - \exp(-\tau M)] + \exp(-\tau M) \left[\cos^k(i) \cos^{k-1}(e) g(\xi) + r(i) \frac{\cos^k(i)}{\Pi} \int_0^{2\pi} \int_0^{\pi/2} \cos^{k-1}(e) g(\xi) \cos e \sin e \, de \, d\psi \right] \cdot [1 + r(e)] \right\} \quad (9)$$

with

$$B = \frac{\rho_0 E_0}{\Pi} \quad A = \frac{3E_0}{16\Pi B}$$

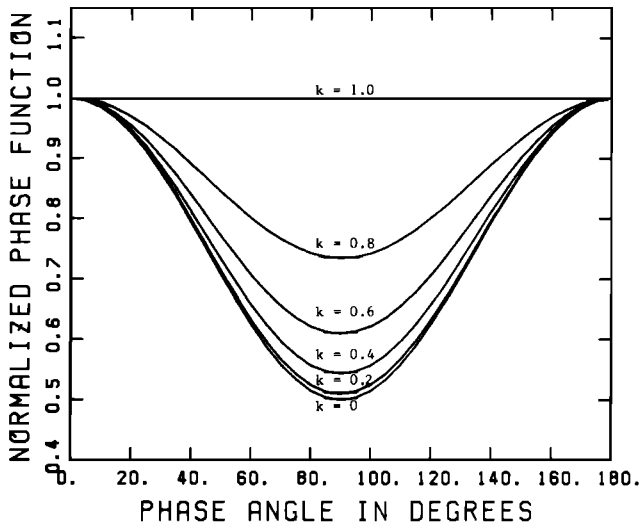


Fig. 1. Normalized phase function for the surface (see equation (11)).

and

$$M = m(i) + m(e)$$

In (9), $g(\xi)$ is the surface phase function which depends on the phase angle ξ , defined as zero when the reflected ray is directed toward the sun. Using (9) in the definition of the anisotropic factors (see equation (2)) it is possible to adjust the parameters k , τ , A simultaneously and to choose a $g(\xi)$ function such that the corresponding factors fit those deduced from the Nimbus 7 ERB experiment. The fit criterion which has been considered here is based on the minimization of the following quantity:

$$DEV(i) = \sum_{n=1}^{n=8} \sum_{p=1}^{p=7} [f_e(i, e, \psi) - f_m(i, e, \psi)]^2 \quad (10)$$

where $f_m(i, e, \psi)$ is the anisotropic factor from Nimbus 7, $f_e(i, e, \psi)$ is the anisotropic factor estimated with (9), and n and p are the indices for azimuth angle increment and satellite angle increment, respectively.

2.4. Results

As mentioned in section 2.2, an investigation of the cases characterized by large solar zenith angles would require a more sophisticated treatment of the atmospheric functions than the one we use here. So for the land regions we have applied this technique for solar zenith angles between 0° and 66°, corresponding to the first six solar bin radiances of the Nimbus 7 data set, and for the desert regions we have studied the whole data set corresponding to solar zenith angles between 0° and 60°. The computation is made with the medium value of each angular bin, and the integration is numerically performed with a Gauss formula. In practice, an estimate for k , τ , and A parameters can be determined easily by plotting and contouring the $DEV(i)$ values as a function of k and A for fixed values of τ . For the determination of the surface phase function $g(\xi)$ the problem is slightly different, and as has already been done by *Hapke* [1963L], we are led to choose and mix scattering curves representative of forward and backward scattering. For the two studied surface types a good fit of the measured data is provided by a simple phase function of the form:

TABLE 1. Fitted Values for τ , A , and k Parameters Over Land and Desert Regions

	Extinction Coefficient τ	Parameter A	Minnaert Parameter κ
Land	0.2	0.9	0.84
Desert	0.2	0.7	0.94

$$g(\xi) = 1 + (1 - k^2) \cos^2(\xi) \quad (11)$$

The corresponding normalized phase function is represented in Figure 1 for different values of k varying between 0 and 1.0. This function leads to maxima of the same intensity in the forward and backward directions and to a relative minimum centered on 90°. A decrease of the k value tends to decrease the intensity in that direction. Although (11) has no theoretical support, it has the advantage of being able to satisfy the reciprocity principle and to parameterize the intrinsic physical state of the surface through the parameter k . The use of an unique surface phase function to describe the reflection characteristics of a given scene for a set of solar angles between 0° and 66° may smooth out the prominent backscatter regime observed by *Salomonson and Marlatt* [1968] and *Davis and Cox* [1982] for intermediate solar angles over desert sands. It must be recalled that we have represented typical clear-sky conditions without aerosols, but when this assumption is not verified, the forward component of the surface phase function we derived can be artificially enhanced.

Values obtained for the parameters k , τ , and A are summarized in Table 1 for land and desert surfaces, respectively. As expected, for the two studied surface types, a good fit is obtained for a low value of the extinction coefficient. Since the desert albedo is higher than the land albedo, we find a comparatively lower value for A over the desert regions. The most interesting feature lies in the values of the parameter k : first, the significant departure from 1.0 indicates a marked anisotropy of the two surface types; second, with a high surface albedo the desert regions are less anisotropic than the land regions. For the two surface types we studied the magnitude of the anisotropic factors is significantly different, but the reflection characteristics are found to be roughly the same. This result can easily be explained by the fact that *Taylor and Stowe's* land category included the desert regions in the total land sampling. However, for intermediate solar angles a great deal of similarities between desert and land surface cases have been observed by *Davis and Cox* [1982] from independent data sets. If this result is confirmed by further extensive studies, it might suggest that the angular patterns of large-scale anisotropic factors are more sensitive to the macrostructure than to the microscattering properties of the sensed surfaces.

Comparisons between the calculated and measured anisotropic factors are illustrated in Figures 2 and 3 for all solar bins over land and desert regions, respectively. For the two studied surface types the correlation coefficient r_c between the two estimates is better than 0.9. However, when the satellite viewing angle is between 75° and 90° (points marked by crosses in Figures 2 and 3), our model overestimates the anisotropic properties of the surface. A possible explanation for this discrepancy is that at large satellite viewing angles, the average functions chosen to describe absorption and scattering significantly underestimate the masking effect of the atmosphere, which acts to smooth out the intrinsic anisotropy of

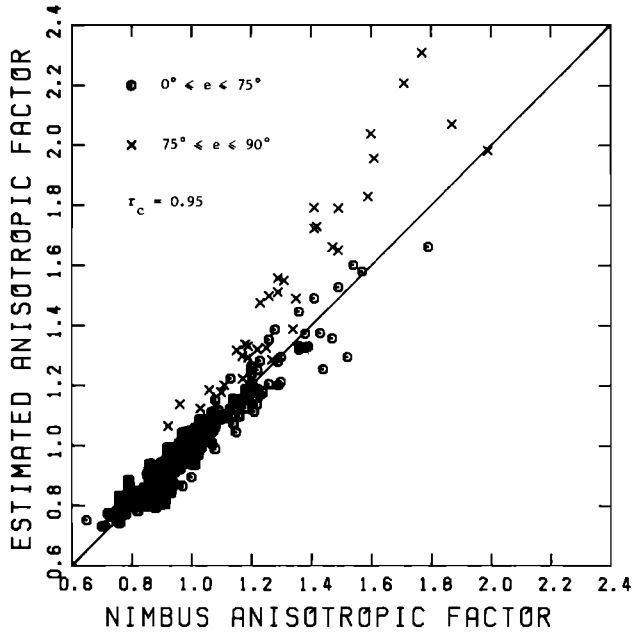


Fig. 2. Comparison between theoretical and measured land anisotropic factors for solar zenith angles between 0° and 66° (circles indicate viewing angles less than 75° and crosses show viewing angles between 75° and 90°).

the sensed surface. The deviation of the points from the bissectrix line can be due to the rather crude modelization we made but may also be due to the intrinsic errors in the anisotropic factors deduced from Nimbus 7. One may expect that this uncertainty mainly comes from the merging of different surface types into a broad category such as land, for instance. An estimate of the intrinsic error can be derived through a first-order development of (2), which leads to

$$\delta f(i, e, \psi) \simeq \bar{f}(i, e, \psi) \frac{\delta L_S(i, e, \psi)}{L_S(i, e, \psi)} [1 - \bar{f}(i, e, \psi)] \quad (12)$$

where $\delta f(i, e, \psi)$ and $\delta L_S(i, e, \psi)$ denote error in anisotropic

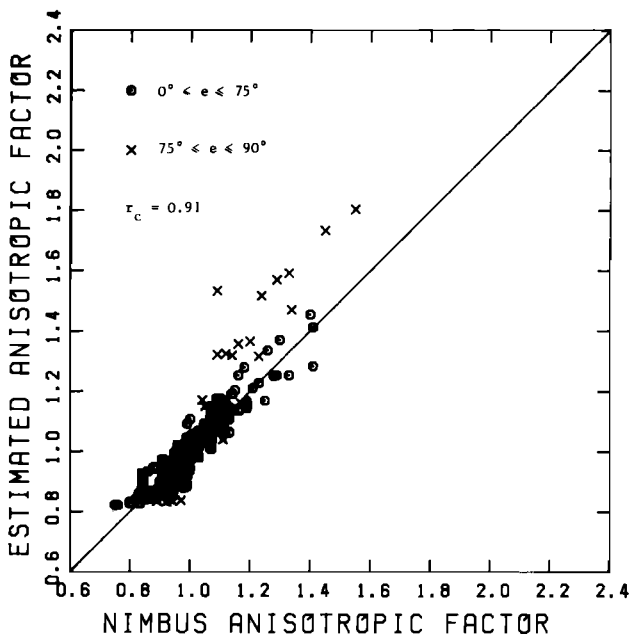


Fig. 3. Same as Figure 2, except over desert regions.

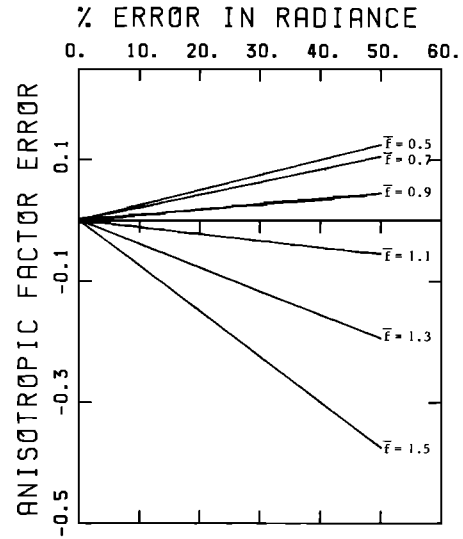


Fig. 4. Estimated errors in Nimbus 7 anisotropic factor versus the relative dispersion (in percent) in measured radiances.

factor and radiance, respectively, and overbars represent spatially averaged values.

Equation (12) is established under the assumption that δL_S is independent of the observational geometry. Figure 4 illustrates the relationship expressed by (12). Taylor and Stowe [1984b] have published values for the relative variation in radiance for each bin. The most common values for this dispersion parameter are located between 20 and 40% for land regions. According to Figure 4, such values lead to uncertainties close to 0.1 and 0.3 in cases where the anisotropic factors are 0.5 and 1.5, respectively. As a matter of fact, the differences between the results from our model and the observations are not larger than the intrinsic errors of these observations.

3. COMPARISON WITH SURFACE ALBEDO MEASUREMENTS

Several experimental studies of the surface boundary layer have emphasized the variation of surface albedos with solar zenith angle (see, for example, Graham and King [1961]; Stew-

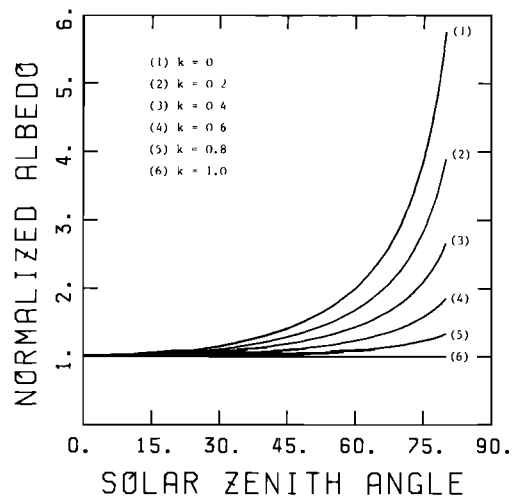


Fig. 5. Variation of normalized surface albedo, with solar zenith angle estimated from (14) for various k values.

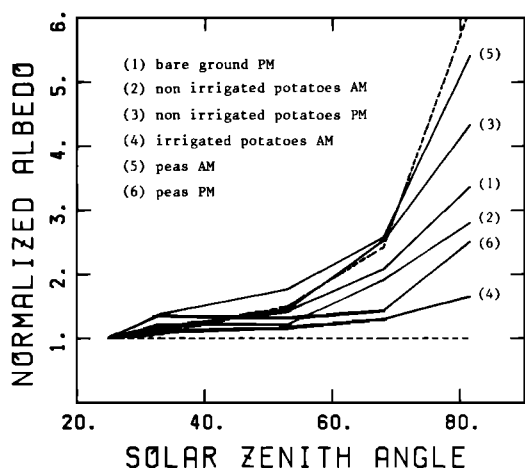


Fig. 6. Variation of normalized surface albedos, with solar zenith angle measured over different surface covers and hours of the day (data from Nkemdirim [1972]). The dashed lines are from (14); $k = 1$ (lower curve) and $k = 0$ (upper curve).

art [1971]; Arnfield [1975]; Idso et al. [1975]). These studies are conducted over parcels with very specific covers, and so the results are representative of a local spatial scale. As expected, the variation of albedo with solar zenith angle is dependent on the surface cover types, and most authors have parameterized the observations with the help of exponential functions. Since the variation of albedo is well documented over some specific surface types, it is valuable to test our surface reflectance model against these observations. The albedo is given by

$$a(i) = \frac{\rho_0}{\pi} \int_0^{2\pi} \int_0^{\pi/2} \cos^{k-1}(i) \cos^{k-1}(e) \cdot [1 + (1 - k^2) \cos^2(\xi)] \cos e \sin e \, de \, d\psi \quad (13)$$

So

$$a(i) = \rho_0 2 \frac{\cos^{k-1}(i)}{k+1} \left\{ 1 + \frac{(1-k^2)}{k+3} [k \cos^2(i) + 1] \right\} \quad (14)$$

The theoretical variation of albedo with solar zenith angle is shown in Figure 5. In this Figure 5 the normalized albedo, that is, $a(i)/a(i=0)$, is reported for different values of k between 0 and 1.0. It can be seen that the dependency of albedo on solar zenith angle increases for low sun and for low k values. The curves of Figure 5 are to be compared to the albedo values published by Nkemdirim [1972] for a variety of surface covers and at different hours of the day (Figure 6). For the sake of comparison the albedo values have been normalized by the albedo measured at the highest sun elevation. In Figure 6 the two dashed lines give the theoretical dependency estimated from (14) at the same solar zenith angles and for k equal to 0 and 1.0, respectively. From this set of experimental curves it appears that with appropriate k values, (14) could provide a good fit of the observations.

4. DISCUSSION AND CONCLUSION

From simple photometric relationships designed for lunar and Martian regions we have derived an analytical expression for the bidirectional reflectances of terrestrial surfaces. This expression has been established with the help of a best fit technique of the anisotropic factors deduced from Nimbus 7 ERB experiment. The proposed model, which satisfies the reci-

procity principle, gives explicitly the form of the bidirectional reflectance for two broad surface categories, one corresponding to land regions and the other corresponding to desert regions.

The main interest in such an expression for the reflectance is to provide a simple support to help understand the anisotropic behavior of currently sensed surfaces. The proposed formulation is also helpful for angular interpolations of existing bidirectional radiance measurements. Obviously, the present model is adapted to describe angular distribution of terrestrial radiances at a spatial scale involved in earth radiation budget studies. Under dust free and cloudless conditions, the main problem lies in the choice of the surface phase function. Although the integrated anisotropic radiance compares favorably with local surface observations, it must be kept in mind that the scattering function used here is not necessarily convenient for specific surface covers. This point must be investigated by using other anisotropic measurements such as those given by Kriebel [1978] and also from future Nimbus 7 data analysis, which should yield anisotropic factors estimated for more specific land categories.

Acknowledgments. The authors would like to express their thanks to C. J. Justus for some valuable discussions on this topic. An anonymous referee produced informative comments which resulted in significant improvements of our paper. The authors thank P. Waldteufel and Y. Pointin for reading the manuscript. The authors are also grateful to C. Paquet and J. Squarise for their dedicated typing and editing of the manuscript.

REFERENCES

- Arnfield, A. J., A note on the diurnal, latitudinal and seasonal variation of the surface reflection coefficient, *J. Appl. Meteorol.*, **14**, 1603-1608, 1975.
- Barkstrom, B. R., The earth radiation budget experiment (ERBE), *Bull. Am. Meteorol. Soc.*, **65**, 1170-1185, 1984.
- Braslau, N., and J. V. Dave, Effects of aerosols on the transfer of solar energy through realistic model atmospheres, 1, Non-absorbing aerosols, *J. Appl. Meteorol.*, **12**, 601-615, 1973.
- Davis, J. M., and S. K. Cox, Reflected solar radiances from regional scale scenes, *J. Appl. Meteorol.*, **21**, 1698-1712, 1982.
- Gillespie, A. R., and A. B. Kahle, Construction and interpretation of a digital thermal inertia image, *Photogramm. Eng. Remote Sens.*, **43**, 983-999, 1977.
- Graham, W. G., and K. M. King, Short-wave reflection coefficient for a field of maize, *Q. J. R. Meteorol. Soc.*, **87**, 425-428, 1961.
- Hapke, B. W., A theoretical photometric function for the lunar surface, *J. Geophys. Res.*, **68**, 4571-4586, 1963.
- Hapke, B. W., and H. Van Horn, Photometric studies of complex surfaces, with applications to the moon, *J. Geophys. Res.*, **68**, 4545-4570, 1963.
- Idso, S. B., R. D. Jackson, R. J. Reginato, B. A. Kimball, and F. S. Nakayama, The dependence of bare soil albedo on soil water content, *J. Appl. Meteorol.*, **14**, 109-113, 1975.
- Jacobowitz, H., H. V. Soule, H. L. Kyle, F. B. House, and the Nimbus 7 ERB Experiment Team, The Earth Radiation Budget (ERB) Experiment: An overview, *J. Geophys. Res.*, **89**, 5021-5038, 1984.
- Kasten, F., A new table and approximate formula for relative optical air mass, *Arch. Meteorol. Geophys. Bioklimatol. Ser. B.*, **14**, 206-223, 1966.
- Kieffer, H. H., T. Z. Martin, A. R. Peterfreund, and B. M. Jakosky, Thermal and albedo mapping of Mars during the Viking primary mission, *J. Geophys. Res.*, **82**, 4249-4291, 1977.
- King, M. D., and B. M. Herman, Determination of the ground albedo and the index of absorption of atmospheric particulates by remote sensing, 1, Theory, *J. Atmos. Sci.*, **36**, 163-173, 1979.
- Kriebel, K. T., Measured spectral bidirectional reflection properties of four vegetated surfaces, *Appl. Opt.*, **17**, 253-259, 1978.
- Minnaert, M., The reciprocity principle in lunar photometry, *Astrophys. J.*, **93**, 403-410, 1941.
- Nkemdirim, L. C., A note on the albedo of surfaces, *J. Appl. Meteorol.*, **11**, 867-874, 1972.

- O'Leary, B., and F. Briggs, Optical properties of Apollo 11 moon samples, *J. Geophys. Res.*, *75*, 6532-6538, 1970.
- Raschke, E., T. H. Vonder Haar, M. Pasternak, and W. R. Bandeen, The radiation balance of the earth-atmosphere system from NIMBUS-3 radiation measurements, *NASA Tech. Note, TN D-7249*, 1973.
- Ruff, I., R. Koffler, S. Fritz, J. S. Winston, and P. K. Rao, Angular distribution of solar radiation reflected from clouds as determined from TIROS IV radiometer measurements, *J. Atmos. Sci.*, *25*, 323-332, 1968.
- Salomonson, V. V., and W. E. Marlatt, Anisotropic solar reflectance over white sand, snow and stratus clouds, *J. Appl. Meteorol.*, *7*, 475-483, 1968.
- Smith, J. A., T. L. Lin, and K. J. Ranson, The Lambertian assumption and Landsat data. *Photogramm. Eng. Remote Sens.*, *46*, 1183-1189, 1980.
- Stephens, G. L., G. G. Campbell, and T. H. Vonder Haar, Earth radiation budgets, *J. Geophys. Res.*, *86*, 9739-9760, 1981.
- Stewart, J. B., The albedo of a pine forest, *Q. J. R. Meteorol. Soc.*, *97*, 561-564, 1971.
- Taylor, V. R., and L. L. Stowe, Reflectance characteristics of uniform earth and cloud surfaces derived from Nimbus-7 ERB, *J. Geophys. Res.*, *89*, 4987-4996, 1984a.
- Taylor, V. R., and L. L. Stowe, Atlas of reflectance patterns for uniform earth and cloud surfaces (Nimbus-7 ERB—61 days), *NOAA Tech. Rep., NESDIS 10*, Natl. Oceanic and Atmos. Admin., Boulder, Colo., 1984b.
- Thorpe, T. E., Viking orbiter photometric observations of the Mars phase function July through November 1976, *J. Geophys. Res.*, *82*, 4161-4165, 1977.
- Veverka, J., and L. Wasserman, Effects of surface roughness on the photometric properties of Mars, *Icarus*, *16*, 281-290, 1972.
- Young, A. T., and S. A. Collins, Photometric properties of the Mariner cameras and of selected regions on Mars, *J. Geophys. Res.*, *76*, 432-437, 1971.
-
- B. Pinty and R. Ramond, Laboratoire Associé de Météorologie Physique/Institut et Observatoire de Physique du Globe, Université de Clermont II, Laboratoire Associé au Centre National de la Recherche Scientifique, No. 267, B.P. 45, 63170 Aubière, France.

(Received June 26, 1985;
revised February 18, 1986;
accepted February 20, 1986.)